

SCIENTIFIC REPORTS



OPEN

A considerable fraction of soil-respired CO₂ is not emitted directly to the atmosphere

Enrique P. Sánchez-Cañete^{1,2,5}, Greg A. Barron-Gafford^{1,3} & Jon Chorover⁴

Soil CO₂ efflux (F_{soil}) is commonly considered equal to soil CO₂ production (R_{soil}), and both terms are used interchangeably. However, a non-negligible fraction of R_{soil} can be consumed in the subsurface due to a host of disparate, yet simultaneous processes. The ratio between CO₂ efflux/O₂ influx, known as the apparent respiratory quotient (ARQ), enables new insights into CO₂ losses from R_{soil} not previously captured by F_{soil} . We present the first study using continuous ARQ estimates to evaluate annual CO₂ losses of carbon produced from R_{soil} . We found that up to 1/3 of R_{soil} was emitted directly to the atmosphere, whereas 2/3 of R_{soil} was removed by subsurface processes. These subsurface losses are attributable to dissolution in water, biological activities and chemical reactions. Having better estimates of R_{soil} is key to understanding the true influence of ecosystem production on R_{soil} as well as the role of soil CO₂ production in other connected processes within the critical zone.

Soil carbon dioxide (CO₂) efflux is the second largest contributor to terrestrial CO₂ exchanges, similar in scale to uptake by terrestrial photosynthesis^{1,2}. Soil CO₂ efflux (F_{soil}) is defined as the rate of CO₂ exchange between soil and atmosphere, and it is the result of soil CO₂ production (R_{soil}) and its transport to the atmosphere. Rates of R_{soil} are the result of heterotrophic respiration during the decomposition of organic matter by microbes and autotrophic respiration by roots³. Both F_{soil} and R_{soil} act together in response to the interactions between biotic and abiotic factors^{4–6}. Generally, F_{soil} increases with the productivity of an ecosystem⁷, driven by increases in temperature and precipitation^{1,8}. With ample water, temperature is the dominant driver of F_{soil} , however, in arid and semiarid ecosystems, patterns of F_{soil} are often driven by precipitation pulses^{9–13} and variation in soil moisture.

F_{soil} can be measured using manual or automatic chambers^{14,15} that capture CO₂ emitted from the soil surface to the atmosphere or estimated by the gradient method through measures of the soil CO₂ molar fraction at multiple depths^{16,17}. Commonly, F_{soil} is considered equal to R_{soil} , and the two terms are used interchangeably within the literature and in land surface models. However, a considerable fraction of the R_{soil} can fail to actually emerge from the soil surface (F_{soil}) due to a host of different processes, such as aqueous phase partitioning¹⁸, calcite dissolution reactions¹⁹, gravitational percolation due to a higher density²⁰, or CO₂ dissolution in xylem water²¹. Therefore, simple estimations of F_{soil} are likely lower than actual rates of R_{soil} . Misrepresenting F_{soil} as R_{soil} can have significant consequences for interpretation of both biotic and abiotic processes because it not only underestimates the contributions of aboveground function to belowground processes, but it also yields a misguided understanding of the rates and drivers of subsurface biogeochemistry and the potential for carbon exports from the system through hydrological transport.

The importance of these alternative CO₂ loss pathways is illustrated when considering that soil can store an order of magnitude greater CO₂ as dissolved inorganic carbon (DIC, inclusive of dissolved CO₂, carbonic acid, bicarbonate, and carbonate) in the aqueous-filled relative to gas-filled pore space²². As a result, large CO₂ losses can be produced by DIC leaching in all ecosystems around the world, with increased CO₂ losses in ecosystems with higher precipitation and higher soil solution pH. In semiarid regions, this DIC leaching may explain a portion of the missing terrestrial carbon sink²³. For this reason, distributed measures of O₂, which has an aqueous solubility 29.7 times lower than CO₂ at 15°C and does not form additional chemical species by dissolution in water, provides a useful constraint on determining soil CO₂ production that might otherwise be missing from R_{soil} .

¹B2 Earthscience, Biosphere 2, University of Arizona, Tucson, 85721, USA. ²Departamento de Física Aplicada, Universidad de Granada, Granada, 18071, Spain. ³School of Geography and Development, University of Arizona, Tucson, 85721, USA. ⁴Department of Soil, Water and Environmental Science, University of Arizona, Tucson, 85721, USA. ⁵IISTA-CEAMA, Instituto Interuniversitario de Investigación del Sistema Tierra en Andalucía, Granada, 18006, Spain. Correspondence and requests for materials should be addressed to E.P.S.-C. (email: enripsc@ugr.es)

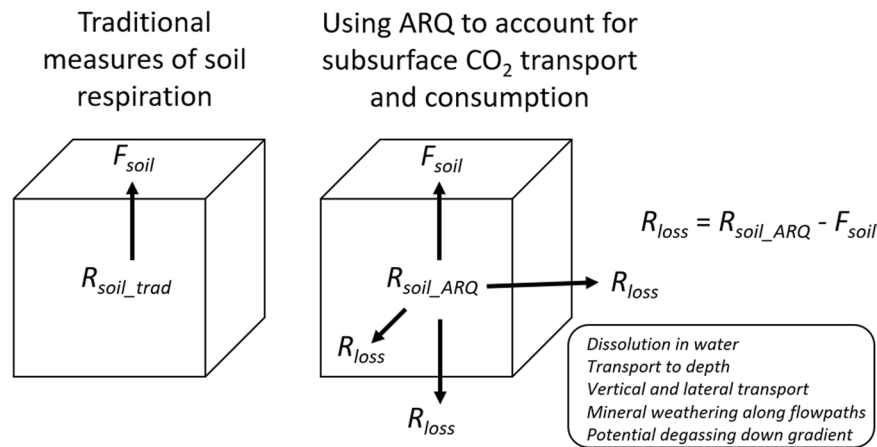


Figure 1. Measurements of *apparent respiratory quotient* (ARQ), i.e., the ratio of soil CO₂ efflux/O₂ influx, have the potential to provide improved quantification of soil respiration, and partitioning of soil respiratory CO₂ into vertical (upward) gaseous and lateral or downward dissolved fluxes. Here, R_{soil} is the soil CO₂ production measured, either using the traditional efflux method (R_{soil_trad}) or on the basis of ARQ (R_{soil_ARQ}). F_{soil} , which is the soil CO₂ (upward) efflux estimated by the CO₂ gradient method, is typically equated to soil respiration (R_{soil_trad}). However, direct continuous measurements of ARQ, as conducted in the current work, reveal that a significant fraction of CO₂ produced by soil respiration is transported or consumed in the subsurface, and not locally emitted to the atmosphere. Hence, a substantial amount of respired CO₂ – unaccounted for by quantifying F_{soil} alone, and denoted here as R_{loss} – can be estimated on the basis of concurrent measures of O₂ influx to soil. The ARQ method reveals a significant component of soil respiration (R_{loss}) that is not emitted locally to the atmosphere. R_{loss} is the CO₂ produced, but unaccounted for, in traditional measures of CO₂ surface efflux. This R_{loss} is consumed by subsurface processes attributable to dissolution in water, vertical and lateral transport along hydrologic flow paths, chemical reactions (including, e.g., silicate and carbonate mineral weathering), and potential degassing upon groundwater discharge (e.g., to streams). Non-negligible values of R_{loss} indicate that (i) flux based measurements alone significantly underestimate local soil respiration and (ii) an important fraction of soil respiratory CO₂ production is consumed in subsurface reactions. R_{soil_ARQ} is the total soil CO₂ production, and the sum of R_{soil} and R_{loss} .

The ratio of soil CO₂ efflux to O₂ influx, known as the *apparent respiratory quotient* (ARQ), allows one to estimate the CO₂ losses from R_{soil} ²². A diagram, with the main variables involved in exchange and loss of CO₂, is shown in Fig. 1. Here we present the first study using continuous ARQ estimates to evaluate annual CO₂ losses of carbon from R_{soil} (R_{soil_ARQ} , where $R_{soil_ARQ} = R_{soil} + R_{loss}$). Our goals were (i) to quantify the values, patterns, and seasonality of ARQ at different soil depths within a semi-arid coniferous forest and then (ii) to estimate the amount of soil CO₂ removed through biological and non-biological processes (R_{soil_ARQ}) (iii) in order to illustrate the disparity between F_{soil} using traditional assumptions that $R_{soil} = F_{soil}$ and an estimate of F_{soil} that takes into account CO₂ losses (R_{loss}) and actual rates of R_{soil} , as determined using the ARQ. Having better estimates of R_{soil} is key to understanding the true influence of aboveground production on R_{soil} , CO₂-induced mineral weathering, and other biologically-driven processes within the critical zone.

Results

The annual time series of climatic and edaphic variables are shown in Fig. 2. During 2015, mean air temperature was 9.4 °C, ranging from –10 to 22 °C with synoptic scale fluctuations driven by atmospheric pressure variations associated with passing of frontal systems (Fig. 2a). Mean soil temperature across all depths was ca. 9.3 °C, with variability decreasing in amplitude with depth (Fig. 2b). Volumetric soil water content (VWC) averaged 20% across all depths with variation over time driven by rainfall events, falling mainly during the monsoon period (typically July–October; Fig. 2c). In 2015, however, the precipitation period extended until mid-November due to an *El Niño* southern oscillation event. The high VWC measured in January–February was due to snowmelt. When precipitation intensity was greater than 3 mm in 30 min, the delay between precipitation and a VWC response was less than 30 min.

Dynamics of the variables considered to control soil gas concentrations and their exchange with the atmosphere are shown in Fig. 2d–g. Mean CO₂ volumetric fraction increased with depth, with average values of 0.25, 0.57 and 0.64% at 10, 30 and 60 cm, respectively. We found a clear annual pattern analogous to the temperature pattern, with maxima in summer and minima in winter. Superimposed on this seasonal trend is pulsed increases in the volumetric fraction of CO₂ driven by precipitation events, with larger amplitude responses during warmer months. Mean O₂ volumetric fraction decreased with increasing depth from 20.27%, to 19.27% and 18.04% at 10, 30 and 60 cm, respectively. The mean O₂ volumetric fraction was significantly different at the three depths, and this difference was sustained through the entire year ($F_{2,336} = 213.9$; $P < 0.05$). Minimum O₂ values occurred in the deepest depths during the snowmelt period, and O₂ variations were anti-correlated with CO₂ at 10 cm (R^2 0.94, $p > 0.05$) and 30 cm (R^2 0.89, $p > 0.05$) throughout the year. However, at 60 cm a poor correlation (R^2 0.11, $p > 0.05$) was found due to the decoupling during the snowmelt. When the snowmelt period (from January 8

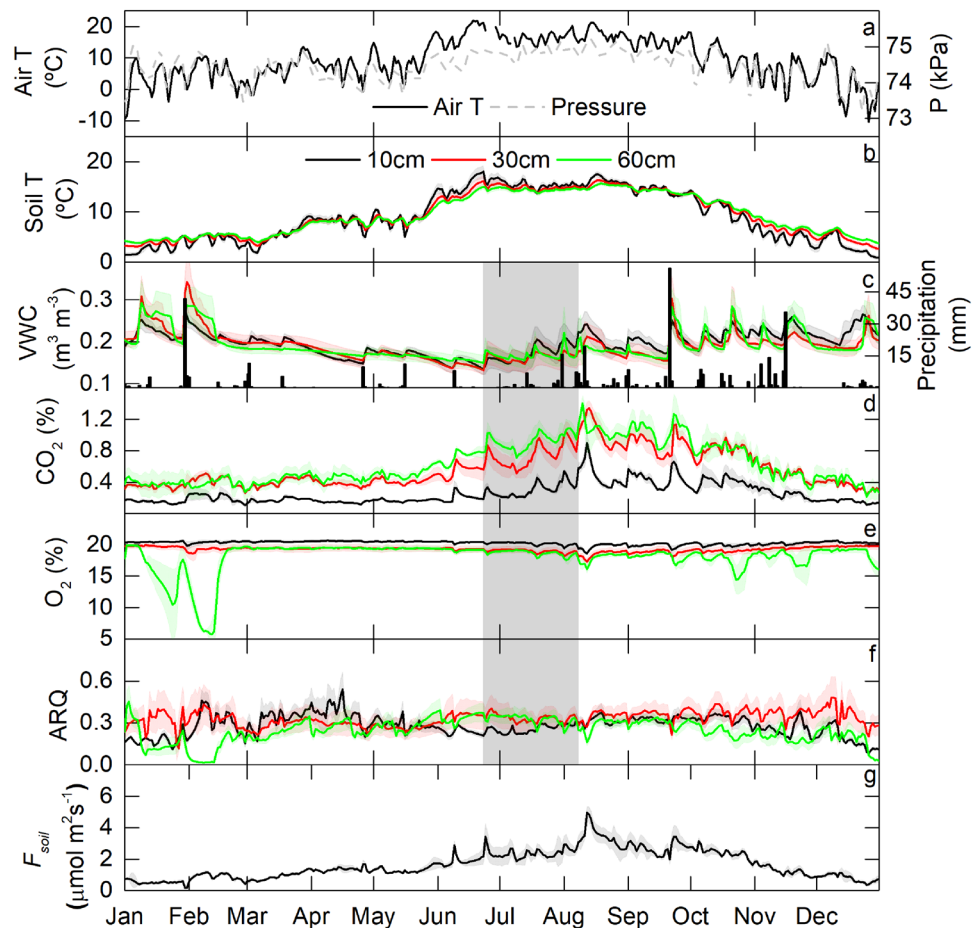


Figure 2. Time series of daily-averaged values for the three pedons of air temperature (Air T), atmospheric pressure (P), soil temperature (Soil T), volumetric water content (VWC), precipitation, CO₂ volumetric fraction, oxygen volumetric fraction, apparent respiratory quotient (ARQ) and soil CO₂ efflux (F_{soil}) at 10, 30, and 60 cm depth during 2015. The standard error for each variable is shown with shading. The period studied in Fig. 2 is highlighted with shading.

to February 20) was excluded from regression analysis, the correlation between O₂ and CO₂ increased notably in deeper layers, with R² values of 0.95, 0.92 and 0.46 at 10, 30 and 60 cm, respectively. Large O₂ fluctuations at 60 cm during the snowmelt period could be due to the snowmelt during daytime producing a wetting front that percolates to lower permeability soil horizons (higher clay content) at depth, stimulation of soil respiration and hence O₂ consumption, but with near saturation conditions limiting diffusion of O₂ into the soil from above. ARQ showed similar mean values at all depths (ca. 0.3), reaching minimum values at 60 cm during snowmelt (January–February) and maximum values at 10 cm in April. F_{soil} was at its maximum during summer and minimum during winter, with an annual mean of 1.64 $\mu\text{mol m}^{-2} \text{s}^{-1}$. Means, standard deviations, minima, maxima, and correlation coefficients for variables shown in Fig. 2 are included in *Supplementary Information* (Tables 1S and 2S). Monthly descriptive statistics for edaphic variables and ARQ are also included there (Fig. 1S).

We also examined, in one soil pedon at 30 min averages, the dynamic behaviour of CO₂ and O₂ through several rain pulse events to capture their combined effects on ARQ (Fig. 3). ARQ slightly increased at 10 cm and 30 cm in response to rain pulses, but remained stable at 60 cm. Interestingly, the rapid increases in CO₂ induced by rain events were counteracted by rapid decreases in O₂, causing only small variations in the ARQ range (c.a. 0.2–0.3). The time to return to values similar to those prior to the precipitation event for CO₂, O₂, ARQ and VWC was not delayed with depth. At 10 cm depth, diurnal ARQ fluctuations showed a higher amplitude than at deeper depths, driven by higher amplitude in the O₂ fluctuations at 10 cm.

The annual cumulative F_{soil} , including consideration of the CO₂ loss (R_{soil_ARQ} , $2012 \pm 223 \text{ gC m}^{-2}$) was 3.2 times higher than traditional estimates of F_{soil} derived using the gradient method ($622 \pm 86 \text{ gC m}^{-2}$, using eq. 1). This suggests that ca. 1400 gC m^{-2} were removed from R_{soil} (Fig. 4) prior to efflux from the soil surface. These ca. 1400 gC m^{-2} represent the soil CO₂ efflux not emitted to the atmosphere (R_{loss}) in the vicinity of production. If R_{soil} was fully emitted to the atmosphere locally, by upward gaseous diffusion processes, with zero R_{loss} , then R_{soil} would accurately reflect F_{soil} . However, this was not the case. The smallest differences between F_{soil} using the traditional assumption of equalling R_{soil} versus using R_{soil_ARQ} were in March, April, September and October, but even then, our recalculated F_{soil} was still 2.7–3.0 times higher (Fig. 4). Maximum differences were produced in January

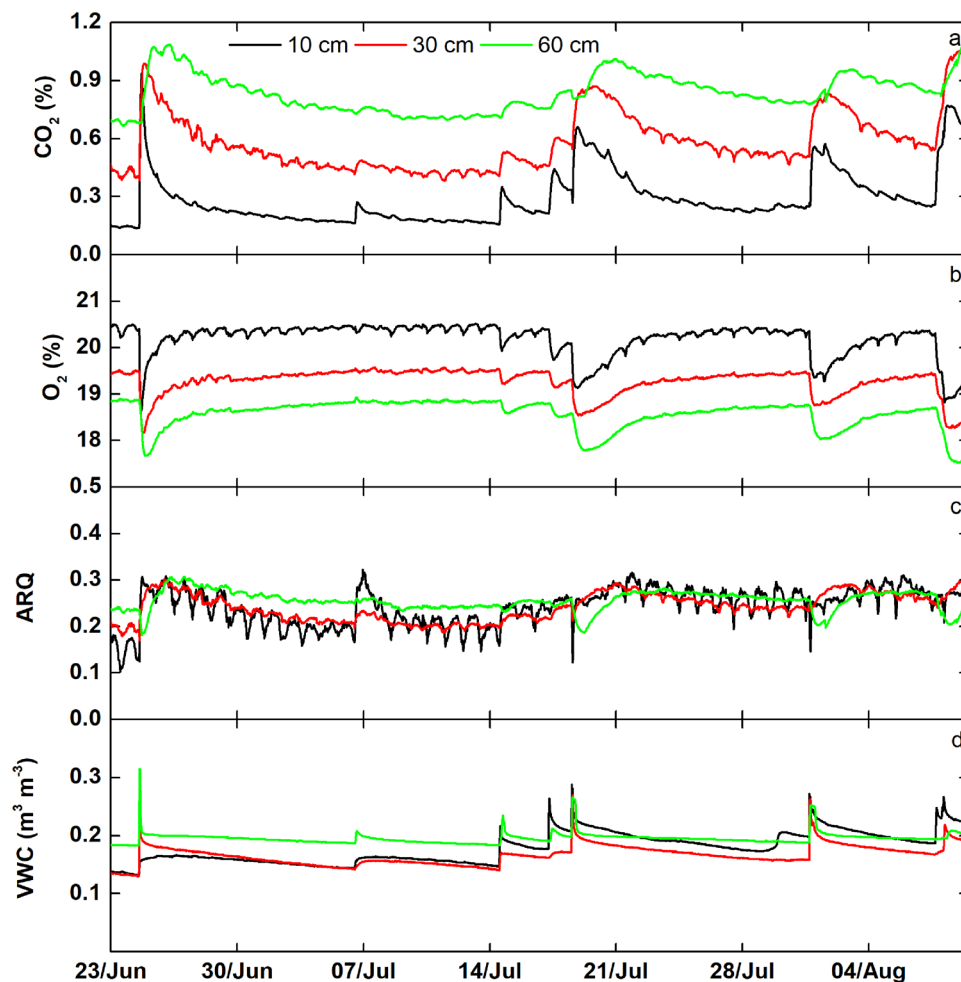


Figure 3. Half-hour averaged values of CO₂ volumetric fraction, O₂ volumetric fraction, apparent respiratory quotient (ARQ) and volumetric water content (VWC) at 10, 30 and 60 depth in a single instrumented pedon (north-facing) during the summer monsoon of 2015.

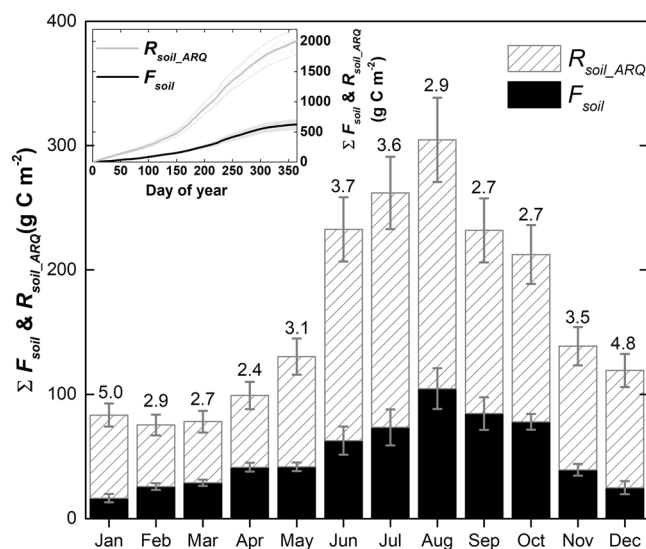


Figure 4. Monthly cumulative soil CO₂ efflux (F_{soil}) (with uncertainty represented as the standard error) and monthly cumulative soil CO₂ efflux, accounting for the CO₂ removed from the soil respiration (R_{soil_ARQ} calculated as R_{soil} multiplied by $0.9 \pm 0.1/ARQ$). The values above of each bar indicate the ratio R_{soil_ARQ}/F_{soil} . The inset figure shows the annual cumulative of F_{soil} and R_{soil_ARQ} and its uncertainty.

and December, when our recalculated F_{soil} was 5.3–5.6 times higher. Our two estimates of F_{soil} (with and without accounting for R_{soil_ARQ}) followed similar monthly patterns despite the differences found in ARQ. The degree of agreement between F_{soil} estimated using the gradient method (Fig. 2g), and periodic chamber measurements of F_{soil} can be found as *Supplementary Information* (Fig. 2S).

Discussion

Given the significant role of soil carbon dynamics in determining other bio-hydro-geochemical processes in the critical zone, there is a need to better understand the dynamic nature of CO₂ production and loss from an ecosystem. The low ARQ values we found here (ARQ ≈ 0.3, Fig. 2 and Table 1S) in comparison to oxidative ratios expected for natural organic matter (i.e., moles of O₂ consumed per mole of CO₂ produced during respiration of organic matter, which average ca. 1.1²⁴ equivalent to ARQ = 0.9), highlight the important role of subsurface biological and non-biological processes in removing CO₂ from R_{soil} . These processes are discussed further below.

If all R_{soil} were emitted directly to the atmosphere by gaseous diffusion processes (that is, if $F_{soil} = R_{soil}$), as is commonly assumed, F_{soil} would be on average approximately three times higher (due to ratio between ARQ theoretical/ARQ measured, 0.9/0.3). Therefore, assuming that all O₂ consumption is associated with respiration, in this semiarid forest only 1/3 of R_{soil} is emitted directly to the atmosphere and 2/3 are removed by subsurface processes. These results are actually quite similar to those found in the only other paper that has calculated *in situ* ARQ for estimates of F_{soil} ²², which reported a mean ARQ of 0.26 and, therefore, an R_{soil} that is 3.8 times higher than F_{soil} estimated in their experimental site (Yatir forest). In that study, researchers collected CO₂ and O₂ samples in a pine forest overlying chalk and limestone bedrock with a mean annual precipitation of 280 mm. Despite their site receiving only 1/3 of the precipitation of our site, and therefore less potential for CO₂ reaction with soil water, a similar ARQ was obtained. This could be attributed to a different composition (and hence oxidative ratio) of the soil organic matter undergoing decomposition, and the effect of CO₂-consuming calcium carbonate dissolution reactions in their soils. Here, we used ARQ = 0.9 as a representative respiratory quotient (RQ) value since it is the mean value corresponding to biomolecular components of natural organic matter²⁴, but if we had used for example the 0.74 value measured for a grassland soil²⁵, the calculated annual F_{soil} would be 1023 g C m⁻², which would be only 1.6 times higher F_{soil} (assuming that all R_{soil} is emitted by diffusion processes). This highlights the fact that the contribution of R_{soil_ARQ} to F_{soil} will depend on the oxidative ratio of the organic matter undergoing degradation, which could potentially change seasonally or with location. Nonetheless, our results are in accordance with Angert *et al.*²² and underscore the important contribution of subsurface processes in removing CO₂ (or O₂) from the soil gas phase prior to its efflux from the soil surface, and the need for a better understanding of the mechanisms involved in those losses.

Prior measurements of RQ have been mostly limited to laboratory experiments using air samples from natural soils or incubated soils, and we do not know of any other studies with *in-situ* and continuous estimates of RQ as a function of soil depth. In our case, assuming that only R_{soil} and diffusion of O₂ and CO₂ give rise to ARQ, ARQ will be equal to RQ and the oxidative ratio (OR) of organic matter undergoing degradation. In this study, the annual mean RQ (calculated as ARQ/0.76) across all depths was 0.38, which was lower than RQ values for some soils ranging from 0.82 to 1^{22,26–29}, but similar to or exceeding those of other soils ranging from 0.21 to 0.40^{22,30–33}. Incubation studies have found a decrease in RQ values with time, often attributed to a depletion of labile organic matter (organic acids and carbohydrates). In such conditions, the microbiota shift to metabolizing less energetically favourable compounds with lower RQ values, such as lipids, lignin and protein³⁴. Therefore, the low RQ values found here might suggest that the carbon in the organic matter undergoing degradation was of relatively low oxidation state. However, RQ values were far lower than the common values of 0.88 for lignin and 0.73 for lipids³⁵, suggesting that low RQ substrates cannot alone explain our results; there must also be CO₂ or O₂ consuming processes contributing to these very low values.

Significant soil CO₂ losses can also be driven by DIC drainage and chemical reactions in the soil. The solubility of CO₂ in water is described by Henry's law, which states that the number of moles of dissolved CO₂ plus carbonic acid per liter of water (collectively referred to as [H₂CO₃*]) are directly proportional to the CO₂ partial pressure and inversely proportional to temperature. In this study, based on aqueous geochemical calculations³⁶, the potential CO₂ removed as DIC during the whole year would be 15.35 g C m⁻². This would represent roughly 2.5% of the cumulative F_{soil} (622 g C m⁻²) and a 1.1% in the C removed from the cumulative R_{loss} (1390 g C m⁻²). These low values of downward DIC transport to groundwater are consistent with the low values of flux estimated globally³⁷. Since they only had individual measurements taken at specific time points, Angert *et al.*²² posited that measurements and considerations of ARQ might become less important on annual and longer timescales when the effects of CO₂ storage and release might be cancelled out. However, using continuous sensing of gas phase composition, we find the opposite. Based on our estimates, when accumulated over an annual time scale, the amount of loss was significant. This may be due, in part, to the complex topography at our mountain site, where the CO₂-enriched water percolates to depth and is then transported laterally to groundwater discharge locations, where it may subsequently degas to the atmosphere directly^{23,38,39}. Indeed, we have observed that the ephemeral stream draining the mountain study site, which runs during snowmelt or intense rainfall events, is in equilibrium with partial pressures of CO₂ that are, on average, 5.4 ± 3.1 times higher than atmospheric⁴⁰. Furthermore, stream discharge of highest [H₂CO₃*] waters is followed a couple of weeks later by a pulse of dissolved silicon derived from rock weathering⁴⁰. With respect to chemical reactions, only those that consume CO₂ or O₂ lead a decrease in RQ. Potential CO₂ consuming reactions include those wherein CO₂ is a reactant in mineral dissolution, such as the dissolution of primary and secondary silicates⁴¹, (oxyhydr)oxides or calcite.

Given that plagioclase is a kinetically labile primary silicate mineral present in the soil profiles of our study site, it is reasonable to expect that some portion of the respired CO₂ is consumed in its weathering to form kaolinite, also observed in our profiles (Table 1). The CO₂-driven weathering of plagioclase to kaolinite consumes two moles of CO₂ per mole of plagioclase. Numerous prior laboratory and field studies have measured rates of

| Depth (cm) | Quartz | Plag-Feldspar | K-Feldspar | Iron Oxides | Mica | 2:1 Clay | 1:1 Clay | Others |
|------------|----------|---------------|------------|-------------|--------------------------------|----------|----------|--------|
| 0–20 | 44.0 | 7.1 | 8.2 | 1.0 | 13.1 | 17.1 | 4.7 | 3.0 |
| 20–40 | 46.2 | 5.8 | 6.9 | 0.5 | 14.2 | 18.5 | 5.9 | 2.3 |
| 40–80 | 40.1 | 4.8 | 6.1 | 0.7 | 13.3 | 16.3 | 5.9 | 4.6 |
| Depth (cm) | Clay (%) | Silt (%) | Sand (%) | pH | Ec ($\mu\text{S}/\text{cm}$) | LOI (%) | | |
| 0–20 | 19.8 | 48.8 | 31.4 | 5.7 | 196.1 | 21.2 | | |
| 20–40 | 27.5 | 44.0 | 28.5 | 5.3 | 199.1 | 5.8 | | |
| 40–80 | 31.8 | 31.4 | 36.8 | 5.1 | 122.1 | 5.0 | | |

Table 1. Soil physicochemical characteristics and mineralogical composition.

plagioclase dissolution at pH values similar to those of the pore waters at our site (ca. pH 5.4). Laboratory-derived weathering rates of plagioclase are typically two to three orders of magnitude higher than those derived from field data (White & Buss, 2014). Hence, whereas steady state laboratory rates are approximately 1.5×10^{-12} moles $\text{m}^{-2} \text{s}^{-1}$, field-measured rates are closer 1×10^{-14} moles $\text{m}^{-2} \text{s}^{-1}$ or lower (normalization in this case is to plagioclase surface area)⁴². Given the mass fraction of plagioclase in the study soils, a soil bulk density of 1.5 g cm^{-3} , and assuming a specific surface area for the plagioclase as $5.6 \text{ m}^2 \text{ g}^{-1}$ (estimated as $3/(\text{particle density} \times \text{particle radius})$)⁴³, we calculate that the steady state rates of plagioclase dissolution could account for consumption of ca. 3.0 to 230 $\text{gC m}^{-2} \text{ y}^{-1}$. Importantly, plagioclase is only one of the primary silicates present in our soils; other labile silicates, such as K-feldspar and mica, will consume comparable quantities of CO_2 during dissolution and both are present at higher mass concentrations. Nonetheless, it seems clear that silicate dissolution alone is unlikely to explain all of the CO_2 removed in our study.

O_2 consuming reactions include the oxidation of Fe(II), NH_4^+ , NO_2^- , mineral sulfides, H_2S and SO_2 ⁴⁴. The rates of pyrite (FeS_2) oxidation in regolith are controlled by the delivery of O_2 to the weathering zone, which consumes 3.75 moles of O_2 per mole of pyrite oxidized, and hence this can be a significant sink for O_2 in soil systems⁴⁵. In our site, this potential contribution may be limited (though not negligible) because of low pyrite content in the schist-derived mineral assemblage. However, biotite (mica) content in our micaceous schist derived soil is significant, representing up to 14% of the bulk soil mineral mass (Table 1), and it can contain up to three moles of Fe(II) per mole of formula, with 0.25 moles of O_2 being consumed per mole of Fe(II) oxidized to Fe(III) during biotite weathering. Although nitrification processes were already considered in the RQ values previously shown, the deposition of calcareous atmospheric dust along with high inputs of Ca^{2+} , Mg^{2+} , K^+ , Na^+ , as found in the region⁴⁶, could have contributed to lowering RQ values due to chemical reactions. Calcite dissolution plays an important role in producing and consuming CO_2 in carbonate-containing soils¹⁹, with one mole of CO_2 consumed per mole of calcite dissolved. The relative contribution of this reaction to subsurface CO_2 consumption is unclear because CaCO_3 does not accumulate to levels quantifiable by X-ray diffraction and soil pH (5.4) is moderately acidic. Nonetheless, the mineralogical and geochemical composition of the soil (Table 1) indicate that all of the previously mentioned reactions could consume CO_2 and O_2 to varying degrees, contributing the low ARQ value we measured here.

Microbial composition likely also impacts the ARQ observed in a given soil. The moles of CO_2 produced per mole of O_2 consumed depends, in part, on the microbial carbon-use efficiency (i.e., the ratio of growth to carbon uptake) of the heterotrophic community⁴⁷. Hence, microbial community composition and environmental conditions (e.g. temperature, tends to decline carbon-use efficiency with increasing temperature) will likewise influence the moles of CO_2 produced per mole of O_2 consumed for a given substrate. The minimum ARQ was obtained at 60 cm during the snowmelt period (Fig. 2f) induced by the minimum O_2 values. However, the maximum ARQ occurred in April. We speculate that this may be the result of the accumulation, over winter, of labile and energetically favourable organic compounds (organic acids and carbohydrates) that are oxidized by a heterotrophic microbial community activated by increasing spring temperatures. Oxidation of such compounds, containing carbon in a higher oxidation state, results in a higher ratio of moles of CO_2 produced per mole of O_2 consumed. Furthermore, chemolithoautotrophic and photoautotrophic organisms can assimilate CO_2 without O_2 production using different metabolic pathways. Photoautotrophic and chemoautotrophic organisms that fix CO_2 and transform it into microbial biomass have been found to be highly abundant in forests⁴⁸, with a global rate for microbial synthesis of organic C of 4.9 to 37.5 $\text{gC m}^{-2} \text{ year}^{-1}$ in different soils⁴⁹. Methanogenic bacteria that metabolize CO_2 to decompose organic matter to CH_4 under anaerobic conditions⁵⁰ have been observed even in well aerated soils such as those found in deserts⁵¹. Therefore, the low ARQ and RQ values found in our soils could indicate one or several processes whereby (i) CO_2 is being removed laterally as dissolved H_2CO_3^* , (ii) CO_2 and O_2 are consumed in geochemical reactions, or (iii) a biological O_2 consumption occurs without emission of CO_2 and *vice versa*.

Subsurface CO_2 consumption has been studied both in soil-atmosphere CO_2 exchanges and in CO_2 exchanges at the ecosystem level. Roland *et al.*⁵² used a chemical carbonate weathering model to explain non-biological fluxes detected at ecosystem scale in a karst, finding that the CO_2 coming from deeper layers at night could be stimulating carbonate dissolution and, thus, consuming CO_2 . Hamerlynck, *et al.*⁵³ found a negative F_{soil} at night in a Chihuahuan desert shrubland, both using an automatic soil chamber and using the gradient method with CO_2 sensors buried in the shallowest layer, similarly attributing the CO_2 consumption to carbonate dissolution. Additionally, temperature influences on the solubility of CO_2 (Henry's Law) were suggested in explaining negative F_{soil} in Antarctic dry valley ecosystems^{54,55}, and soil electrical conductivity and pH were correlated with CO_2 uptake in alkaline desert soils⁵⁶. All of these studies found negative F_{soil} , highlighting that CO_2 consumptive processes in the soil were higher than CO_2 production processes. This is not unexpected in such ecosystems,

where R_{soil} is very low due to low biological activity and therefore even small changes in R_{soil} can change the sign of the soil-atmosphere CO_2 gradient. In our ecosystem, F_{soil} was always positive, but the complementary O_2 measurements provided a novel insight, confirming that even in ecosystems with high biological production, non-biological processes are masked by high R_{soil} and therefore, are difficult to detect from F_{soil} measurements alone.

In conclusion, this study highlights the important and dynamic, but often overlooked, roles played by sub-surface transport and weathering processes that differentiate R_{soil} from surface measures or estimates of F_{soil} . As Angert *et al.*²² noted, variations in the ARQ in acidic and neutral soils (as we have here) are likely tied to substrates and processes not well understood at present, and such processes warrant further research. Therefore, we must change our point of view regarding R_{soil} studies from an inappropriately conceived system in which all CO_2 is produced by biology, to a dynamic system where the soil CO_2 is produced and removed by the interaction of combinatorial biological processes, hydrologic transport, and associated geochemical reactions. Because the fraction of R_{soil} contributing to F_{soil} depends on the ARQ chosen, we recommend that future F_{soil} studies use a combination of soil CO_2 and O_2 sensors to determine ARQ values. Such an approach can yield important information to quantify the CO_2 removed by biological and non-biological processes. ARQ and RQ values are key in estimating CO_2 sinks deduced from changes in atmospheric O_2 concentration⁵⁷ and are highly influential in evaluating ecosystem productivity. Currently, ecosystem productivity is estimated using values of net ecosystem exchange, as the sum of gross primary production (GPP) and ecosystem respiration (R_{eco}). This may be problematic because that R_{eco} consists of an aboveground component attributed to plant respiration and a belowground component, F_{soil} that we now know may incompletely quantify soil respiration. In our ecosystem, if soil CO_2 losses were calculated from F_{soil} alone, GPP estimates would be erroneously low, and if this is consistent across other ecosystems, it could have enormous implications on carbon exchange studies from ecosystem to global scale.

Material and Methods

Site description. The field site is a mixed conifer forest located at 2573 m a.s.l. on Mt. Bigelow north of Tucson, Arizona, in the Santa Catalina Mountains-Jemez River Basin Critical Zone Observatory⁵⁸. The climate is semi-arid, with a mean annual temperature of 9.4 °C and mean annual precipitation of 750 mm, falling mostly during the summer monsoon. Snow falls during winter, usually persisting from December to March. Ponderosa pine (*Pinus ponderosa*) and Douglas fir (*Pseudotsuga menziesii*) dominate the site with a mean canopy height of 10 m. The soil has a sandy loam texture of 32.3% sand, 41.4% silt and 26.4% clay with a pH of 5.4 and a depth to bedrock of ca. 1 m. Additional information about mineral composition and other soil properties can be found in Table 1.

Experimental design. Field measurements were conducted during the complete calendar year of 2015. Three instrumented pedons were equipped to measure each of the following, using co-located sensors: temperature and humidity (5 TM, Decagon, USA), O_2 molar fraction (SO-110, Apogee, USA; Manufacturer reports a sensitivity of 26 μV per 0.01% and repeatability < 0.1% of reading), and CO_2 molar fraction at 10, 30 and 60 cm depth. A drift correction was applied to the O_2 sensors assuming a constant linear signal decrease as the manufacturer reported (1 mV per year). The measurement range of the CO_2 sensors was up to 10,000 ppm at 10 cm and 20,000 ppm at 30 and 60 cm (GMM222 and GMM221, Vaisala, Finland; accuracy 1.5%, repeatability 2% of reading). Both CO_2 and O_2 values were corrected for variations in temperature, humidity, and pressure per instructions from the manufacturer. Atmospheric pressure, air temperature, and precipitation were obtained from a meteorological tower. Data-loggers (CR1000, Campbell scientific, USA) collected measurements every 30 s and stored 30 min averages. The instrumented pedons are separated from each other by distances of ca. 10 meters, and they are located, respectively, on a south facing slope, a north facing slope, and in a convergent valley position within a zero order basin. One-way ANOVA for mean values of soil temperature, soil water content, CO_2 and O_2 between 3 pedons at 3 depths, showed significant differences among all the means at each depth for each variable. Here, we aggregated the three pedons and analysed the average values and their standard error to show the uncertainty in the spatial variability.

Procedure to estimate F_{soil} . Estimates of F_{soil} were obtained using the gradient method through the equation⁵⁹:

$$F_{soil} = -\rho k_s \frac{\partial c}{\partial x} \quad (1)$$

where F_{soil} ($\mu mol CO_2 m^{-2} s^{-1}$), ρ is the air density ($mol air m^{-3}$), ∂c is the CO_2 molar fraction gradient ($\mu mol CO_2 mol air^{-1}$) calculated using the difference between atmospheric CO_2 molar fraction (400 ppm) and the CO_2 value at 10 cm depth, ∂x is the vertical gradient (m) and k_s is the *in situ* CO_2 transfer coefficient ($m^2 s^{-1}$) obtained by rearranging Eq. 1:

$$k_s = -\frac{F_{chamber} \partial x}{\rho \partial c} \quad (2)$$

where $F_{chamber}$ was measured by a portable soil CO_2 efflux chamber (Li-8100, Li-Cor, USA) from 18 collars around the instrumented pedons, follow a transect from the south face to the north face going through the valley, every two weeks during the months without snow cover ($n=20$). Later, k_s was modelled using a power function ($k_s/D_a = a \theta_a^b$) of the soil air porosity ($\theta_a =$ soil porosity-soil water content), where D_a is the diffusion coefficient of CO_2 in free air ($m^2 s^{-1}$) and a and b are coefficients obtained by least squares regression.

Procedure to estimate ARQ. The ratio of soil CO₂ efflux to soil O₂ influx, designated as apparent respiratory quotient (ARQ), was estimated following Angert *et al.*²²:

$$ARQ = \frac{F_{CO_2}}{F_{O_2}} = \frac{-\rho D_{s_{CO_2}} \frac{\partial c}{\partial z}}{-\rho D_{s_{O_2}} \frac{\partial o}{\partial z}} \quad (3)$$

simplifying,

$$ARQ = \frac{-D_{s_{CO_2}} \frac{\partial c}{\partial o}}{-D_{s_{O_2}}} = -0.76 \frac{\partial c}{\partial o} \quad (4)$$

where the constant “0.76” is derived from the ratio of CO₂/O₂ diffusion coefficients in air, ∂c is the CO₂ molar fraction gradient calculated using the discrete difference between the atmosphere and the CO₂ value at each depth and ∂o is the O₂ molar fraction gradient calculated using the difference between atmosphere and the O₂ value at each depth. Consumption of either soil CO₂ or soil O₂ will decrease the ARQ; consumption of soil CO₂ decreases the difference in the numerator (∂c) and hence decreases ARQ, whereas consumption of soil O₂ increases the difference represented in the denominator (∂o), and hence also decreases ARQ.

ARQ values have previously only been reported by Angert *et al.*²², who found that ARQ ranged from 0.14–1.23 across six different experimental sites. Most previous studies have focused either on the *respiratory quotient* (RQ), defined as the moles of CO₂ produced per mole of O₂ consumed during R_{soil} , or the *oxidative ratio* (OR), defined as moles of O₂ consumed per mole CO₂ produced (i.e., 1/RQ). Therefore, if we assume that only R_{soil} drives ARQ, it will be equal to RQ or 1/OR.

The natural biochemical variation in RQ is large depending on the kind of compound undergoing oxidation, ranging from (mean values reported for each biomolecular type) 1.47 for organic acids, 1.00 for carbohydrates, 0.95 for soluble phenolics, 0.88 for proteins and lignins, and 0.73 for lipids (OR values in Randerson *et al.*,³⁵). From stoichiometric considerations, mean RQ values were calculated as 0.95 for different types of wood and 0.89 for humic acid and humin (OR values in Severinghaus²⁸). In soils, RQ values have been reported to vary from 0.83–0.95 for different biomes inside Biosphere 2²⁸, 0.82–1.04 for Boreal, Temperate Subtropical and Mediterranean ecosystems²⁹, 0.90 in a cool temperate deciduous forest²⁷, and a mean value of 1 in the Amazonian tropical forest²⁶. Therefore, based on previous research, an ARQ value of *ca.* 0.9 ± 0.1 is consistent with R_{soil} and diffusion processes alone. However, ARQ values below this would indicate removal of CO₂ or O₂ by non-respiratory processes²². Therefore, assuming both abiotic O₂ removal and autotrophic microorganisms in the soil are negligible, to estimate the F_{soil} taking into account the CO₂ loss from the soil, one can multiply R_{soil} (or F_{soil} assuming that all R_{soil} is emitted to the atmosphere by gaseous diffusion processes, and therefore, $F_{soil} = R_{soil}$) by 0.9 ± 0.1 /ARQ, as was done in the current study and previously by Angert *et al.*²².

References

1. Raich, J. W. & Schlesinger, W. H. The global carbon dioxide flux in soil respiration and its relationship to vegetation and climate. *Tellus B* **44**, 81–99 (1992).
2. Schimel, D. S. *et al.* Recent patterns and mechanisms of carbon exchange by terrestrial ecosystems. *Nature* **414**, 169–172 (2001).
3. Hogberg, P. *et al.* Large-scale forest girdling shows that current photosynthesis drives soil respiration. *Nature* **411**, 789–792 (2001).
4. Buchmann, N. Biotic and abiotic factors controlling soil respiration rates in *Picea abies* stands. *Soil Biol. Biochem.* **32**, 1625–1635 (2000).
5. Xu, W. & Wan, S. Water- and plant-mediated responses of soil respiration to topography, fire, and nitrogen fertilization in a semiarid grassland in northern China. *Soil Biol. Biochem.* **40**, 679–687 (2008).
6. Curiel Yuste, J., Nagy, M., Janssens, I. A., Carrara, A. & Ceulemans, R. Soil respiration in a mixed temperate forest and its contribution to total ecosystem respiration. *Tree Physiol.* **25**, 609–619 (2005).
7. Bahn, M. *et al.* Soil Respiration in European Grasslands in Relation to Climate and Assimilate Supply. *Ecosystems* **11**, 1352–1367 (2008).
8. Bahn, M. *et al.* Soil respiration at mean annual temperature predicts annual total across vegetation types and biomes. *Biogeosciences* **7**, 2147–2157 (2010).
9. Huxman, T. E. *et al.* Precipitation pulses and carbon fluxes in semiarid and arid ecosystems. *Oecologia* **141**, 254–268 (2004).
10. Sponseller, R. A. Precipitation pulses and soil CO₂ flux in a Sonoran Desert ecosystem. *Glob. Chang. Biol.* **13**, 426–436 (2007).
11. Vargas, R. *et al.* Precipitation variability and fire influence the temporal dynamics of soil CO₂ efflux in an arid grassland. *Glob. Chang. Biol.* **18**, 1401–1411 (2012).
12. Barron-Gafford, G. A., Scott, R. L., Jenerette, G. D. & Huxman, T. E. The relative controls of temperature, soil moisture, and plant functional group on soil CO₂ efflux at diel, seasonal, and annual scales. *J. Geophys. Res.* **116** (2011).
13. Barron-Gafford, G. A. *et al.* Quantifying the timescales over which exogenous and endogenous conditions affect soil respiration. *New Phytol.* **202**, 442–454 (2014).
14. Savage, K. E. & Davidson, E. A. A comparison of manual and automated systems for soil CO₂ flux measurements: trade-offs between spatial and temporal resolution. *J. Exp. Bot.* **54**, 891–899 (2003).
15. Pumpanen, J. *et al.* Comparison of different chamber techniques for measuring soil CO₂ efflux. *Agric. For. Meteorol.* **123**, 159–176 (2004).
16. Davidson, E. A. & Trumbore, S. E. Gas diffusivity and production of CO₂ in deep soils of the Eastern Amazon. *Tellus Series B/Chemical and Physical Meteorology* **47**, 550–565 (1995).
17. Maier, M. & Schack-Kirchner, H. Using the gradient method to determine soil gas flux: A review. *Agric. For. Meteorol.* **192**, 78–95 (2014).
18. Kern, D. M. The hydration of carbon dioxide. *J. Chem. Educ.* **37**, 14 (1960).
19. Serrano-Ortiz, P. *et al.* Hidden, abiotic CO₂ flows and gaseous reservoirs in the terrestrial carbon cycle: Review and perspectives. *Agric. For. Meteorol.* **150**, 321–329 (2010).
20. Sánchez-Cañete, E. P., Serrano-Ortiz, P., Domingo, F. & Kowalski, A. S. Cave ventilation is influenced by variations in the CO₂-dependent virtual temperature. *Int. J. Speleol.* **42**, 1–8 (2013).
21. Aubrey, D. P. & Teskey, R. O. Root-derived CO₂ efflux via xylem stream rivals soil CO₂ efflux. *New Phytol.* **184**, 35–40 (2009).

22. Angert, A. *et al.* Using O₂ to study the relationships between soil CO₂ efflux and soil respiration. *Biogeosciences* **12**, 2089–2099 (2015).
23. Li, Y., Wang, Y. G., Houghton, R. A. & Tang, L. S. Hidden carbon sink beneath desert. *Geophys. Res. Lett.* **42**, 5880–5887 (2015).
24. Masiello, C. A., Gallagher, M. E., Randerson, J. T., Deco, R. M. & Chadwick, O. A. Evaluating two experimental approaches for measuring ecosystem carbon oxidation state and oxidative ratio. *J. Geophys. Res. Biogeosciences* **113** (2008).
25. Worrall, F., Clay, G. D. & Macdonald, A. The impact of fertilizer management on the oxidation status of terrestrial organic matter. *Soil Use Manag.* **32**, 45–52 (2016).
26. Angert, A. *et al.* Internal respiration of Amazon tree stems greatly exceeds external CO₂ efflux. *Biogeosciences* **9**, 4979–4991 (2012).
27. Ishido, S. *et al.* O₂: CO₂ exchange ratios observed in a cool temperate deciduous forest ecosystem of central Japan. *Tellus B* **65** (2013).
28. Severinghaus, J. P. *Studies of the Terrestrial O₂ and Carbon Cycles in Sand Dune Gases and in Biosphere 2.* Columbia University (1995).
29. Hockaday, W. C. *et al.* Measurement of soil carbon oxidation state and oxidative ratio by ¹³C nuclear magnetic resonance. *J. Geophys. Res. Biogeosciences* **114** (2009).
30. Dilly, O. Microbial respiratory quotient during basal metabolism and after glucose amendment in soils and litter. *Soil Biol. Biochem.* **33**, 117–127 (2001).
31. Aon, M. A., Sarena, D. E., Burgos, J. L. & Cortassa, S. Interaction between gas exchange rates, physical and microbiological properties in soils recently subjected to agriculture. *Soil Tillage Res.* **60**, 163–171 (2001).
32. Dilly, O. Regulation of the respiratory quotient of soil microbiota by availability of nutrients. *FEMS Microbiol. Ecol.* **43**, 375–381 (2003).
33. Cortassa, S., Aon, M. A. & Villon, P. F. A method for quantifying rates of O₂ consumption and CO₂ production in soil. *Soil Sci.* **166**, 68–77 (2001).
34. Carlile, M. J., Watkinson, S. C. & Gooday, G. W. *The Fungi.* <https://doi.org/10.1016/B978-012738445-0/50021-6> (2001)
35. Randerson, J. T. *et al.* Is carbon within the global terrestrial biosphere becoming more oxidized? Implications for trends in atmospheric O₂. *Glob. Chang. Biol.* **12**, 260–271 (2006).
36. Stumm, W. & Morgan, J. J. *Aquatic Chemistry: Chemical Equilibria and Rates in Natural Waters.* John Wiley & Sons (John Wiley and Sons, 1993).
37. Kessler, T. J. & Harvey, C. F. The global flux of carbon dioxide into groundwater. *Geophys. Res. Lett.* **28**, 279 (2001).
38. López-Ballesteros, A. *et al.* Subterranean ventilation of allochthonous CO₂ governs net CO₂ exchange in a semiarid Mediterranean grassland. *Agric. For. Meteorol.* **234–235**, 115–126 (2017).
39. Perdrial, J. N. *et al.* Stream water carbon controls in seasonally snow-covered mountain catchments: Impact of inter-annual variability of water fluxes, catchment aspect and seasonal processes. *Biogeochemistry* **118**, 273–290 (2014).
40. Chorover, J. *et al.* Biogeochemical control points in a water-limited critical zone. in *Annual Meeting of the American Geophysical Union* (2017).
41. Berner, R. A., Lasaga, A. C. & Garrels, R. M. The carbonate-silicate geochemical cycle and its effect on atmospheric carbon dioxide over the past 100 million years. *American Journal of Science* **283**, 641–683 (1983).
42. White, A. F. & Buss, H. L. In 115–155 BT–Treatise on Geochemistry, <https://doi.org/10.1016/B978-0-08-095975-7.00504-0> (Amsterdam:Elsevier, 2014).
43. Pennell, K. D. In *Methods of Soil Analysis: Part 4 Physical Methods* 295–315, <https://doi.org/10.2136/sssabookser5.4.c13> (Soil Science Society of America, 2002).
44. Mulder, J. & Cresser, M. S. In *Biogeochemistry of Small Catchments: A tool for Environmental Research* (eds Moldan, B. & Cerny, J.) 207–228 <https://doi.org/10.1029/93WR02950> (John Wiley & Sons, 1994).
45. Binning, P. J., Postma, D., Russell, T. F., Wesselingh, J. A. & Boulin, P. F. Advective and diffusive contributions to reactive gas transport during pyrite oxidation in the unsaturated zone. *Water Resour. Res.* **43** (2007).
46. Sorooshian, A. *et al.* Aerosol and precipitation chemistry in the southwestern United States: spatiotemporal trends and interrelationships. *Atmos. Chem. Phys.* **13**, 7361–7379 (2013).
47. Manzoni, S., Taylor, P., Richter, A., Porporato, A. & Ågren, G. I. Environmental and stoichiometric controls on microbial carbon-use efficiency in soils. *New Phytologist* **196**, 79–91 (2012).
48. Tolli, J. & King, G. M. Diversity and structure of bacterial chemolithotrophic communities in pine forest and agroecosystem soils. *Appl. Environ. Microbiol.* **71**, 8411–8418 (2005).
49. Yuan, H. *et al.* Microbial autotrophy plays a significant role in the sequestration of soil carbon. *Appl. Environ. Microbiol.* **78** (2012).
50. Stevens, S. H., Ferry, J. G. & Schoell, M. *Methanogenic Conversion of CO₂ Into CH₄.* (Advanced Resources International, Inc., 2012).
51. Peters, V. & Conrad, R. Methanogenic and other strictly anaerobic bacteria in desert soil and other oxic soils. *Appl. Environ. Microbiol.* **61**, 1673–1676 (1995).
52. Roland, M. *et al.* Atmospheric turbulence triggers pronounced diel pattern in karst carbonate geochemistry. *Biogeosciences* **10**, 5009–5017 (2013).
53. Hamerlynck, E. P., Scott, R. L., Sánchez-Cañete, E. P. & Barron-Gafford, G. A. Nocturnal soil CO₂ uptake and its relationship to subsurface soil and ecosystem carbon fluxes in a Chihuahuan Desert shrubland. *J. Geophys. Res.* **118**, 1593–1603 (2013).
54. Parsons, A. N., Barrett, J. E., Wall, D. H. & Virginia, R. A. Soil Carbon Dioxide Flux in Antarctic Dry Valley Ecosystems. *Ecosystems* **7**, 286–295 (2004).
55. Ball, B. A., Virginia, R. A., Barrett, J. E., Parsons, A. N. & Wall, D. H. Interactions between physical and biotic factors influence CO₂ flux in Antarctic dry valley soils. *Soil Biol. Biochem.* **41**, 1510–1517 (2009).
56. Xie, J., Li, Y., Zhai, C., Li, C. & Lan, Z. CO₂ absorption by alkaline soils and its implication to the global carbon cycle. *Environ. Geol.* **56**, 953–961 (2009).
57. Keeling, R. F., Piper, S. C. & Heimann, M. Global and hemispheric CO₂ sinks deduced from changes in atmospheric CO₂ concentration. *Nature* **381**, 218–221 (1996).
58. Potts, D. L., Minor, R. L., Braun, Z. & Barron-Gafford, G. A. Photosynthetic phenological variation may promote coexistence among co-dominant tree species in a Madrean sky island mixed conifer forest. *Tree Physiol.* **37**, 1229–1238 (2017).
59. Sánchez-Cañete, E. P., Scott, R. L., van Haren, J. & Barron-Gafford, G. A. Improving the accuracy of the gradient method for determining soil carbon dioxide efflux. *J. Geophys. Res. Biogeosciences* **122**, 50–64 (2017).

Acknowledgements

This project and data were supported by NSF awards 1417101 and 1331408, as well as by the European Commission project DIESEL (FP7-PEOPLE-2013-IOF, 625988) and the Spanish Ministry of Economy and Competitiveness (IJCI-2016-30822). All data used in this study are freely available (<http://criticalzone.org/catalina-jemez/data/datasets/>). The authors wish to thank Rebecca Larkin Minor and Nate Abramson for their careful operation and maintenance of the field measurement devices. The program “Unidades de Excelencia Científica del Plan Propio de Investigación de la Universidad de Granada” funded the cost of this publication.

Author Contributions

G.A.B-G. and J.C. conceived and designed the research. E.P.S.-C. analysed the data, prepared tables and figures and wrote the draft manuscript. E.P.S.-C., G.A.B-G. and J.C. wrote the paper.

Additional Information

Supplementary information accompanies this paper at <https://doi.org/10.1038/s41598-018-29803-x>.

Competing Interests: The authors declare no competing interests.

Publisher's note: Springer Nature remains neutral with regard to jurisdictional claims in published maps and institutional affiliations.



Open Access This article is licensed under a Creative Commons Attribution 4.0 International License, which permits use, sharing, adaptation, distribution and reproduction in any medium or format, as long as you give appropriate credit to the original author(s) and the source, provide a link to the Creative Commons license, and indicate if changes were made. The images or other third party material in this article are included in the article's Creative Commons license, unless indicated otherwise in a credit line to the material. If material is not included in the article's Creative Commons license and your intended use is not permitted by statutory regulation or exceeds the permitted use, you will need to obtain permission directly from the copyright holder. To view a copy of this license, visit <http://creativecommons.org/licenses/by/4.0/>.

© The Author(s) 2018